FE-Characterisation vs. Experimental Analysis of a Brushless DC Automotive Actuator

Dr. Dorin ILES
R&D Lab for Electric Drives
ebm-papst St. Georgen GmbH, Germany

Objectives:

1. FE-analysis using JMAG was carried out determining all relevant characteristics for a (6+6) slot/8 pole, 3 phase interior permanent magnet (IPM) brushless D.C. motor considered as a proper candidate for an automotive actuator application

2. Experimental analysis is described and the measurement results are presented and whenever possible compared with computational results, in order to validate the FEM-computations for this type of machine

Outline of presentation:

- **Section I**. Introduction.
- **Section II.** IPM BLDC.
  - **A.** Defining the case study.
  - **B.** Materials, construction and manufacturing technologies.
- **Section III.** FEM characterization of BLDC using JMAG.
  - **A.** Cogging torque calculation.
  - **B.** No-load flux linkage and back-emf.
  - **C.** Load torque.
  - **D.** Computation of inductances.
- **Section IV.** Experimental analysis of IPMBLDC.
  - **A.** Phase resistance measurement.
  - **B.** Phase self and line-to-line inductance measurement.
  - **C.** Standstill torque measurement.
  - **D.** Phase back-emf measurement.
  - **E.** Cogging torque measurement.
  - **F.** Friction and iron loss torque versus speed.
- **Section V.** Conclusion.

I. Introduction

Automotive electric drives – an overview

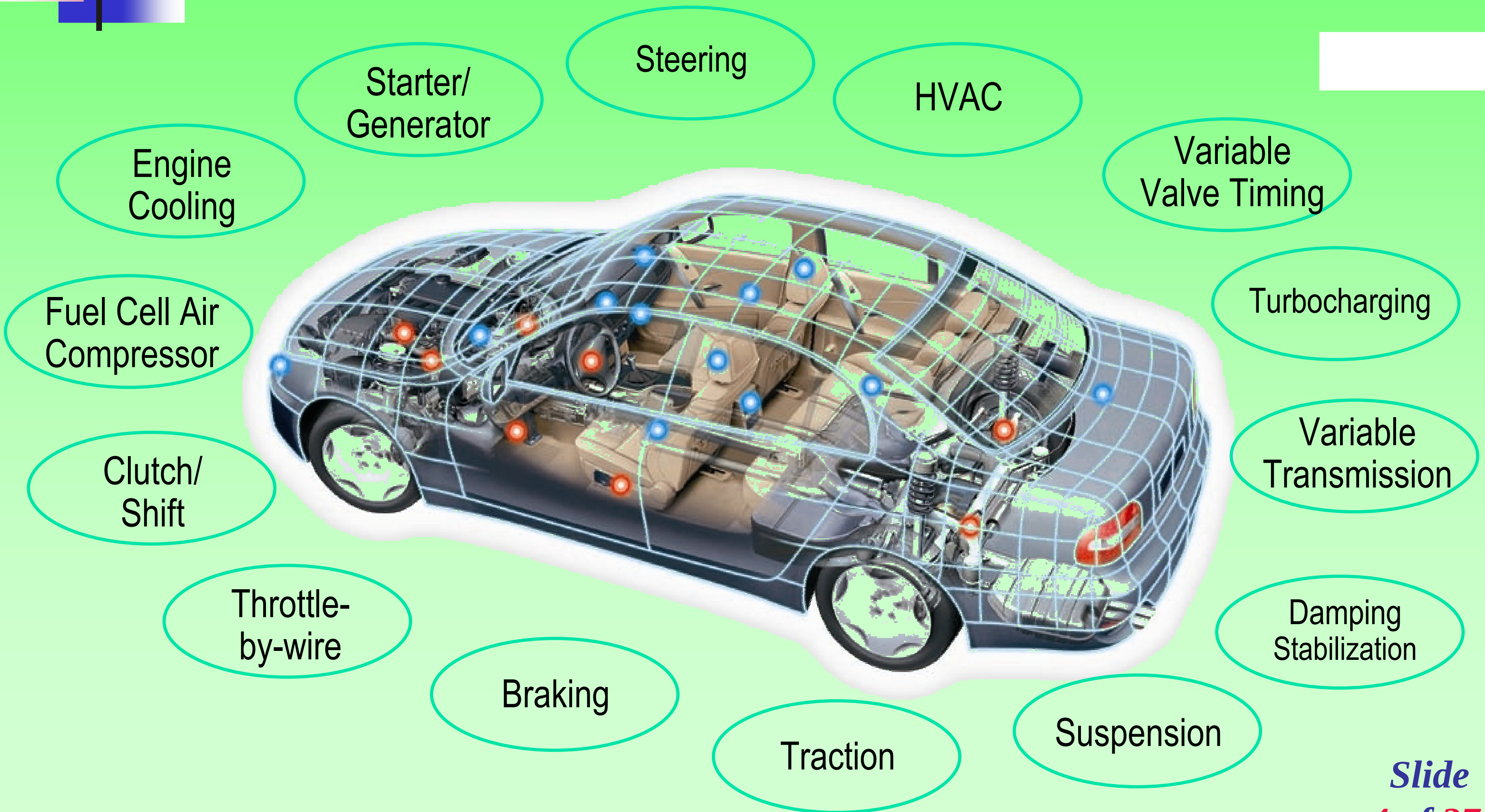

I. Introduction

Automotive electric drives – torque-speed demands

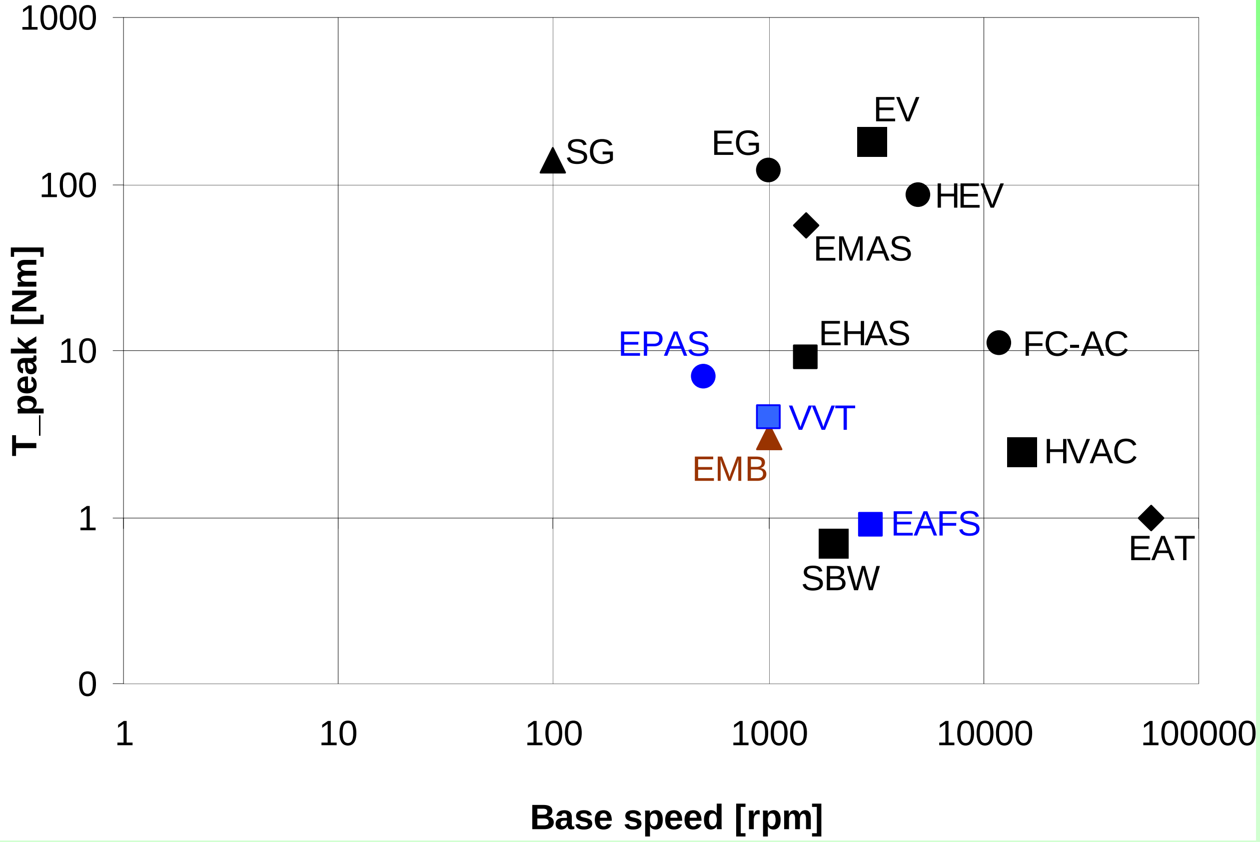

Application	Description
EPAS	Electric power assisted steering
EAFS	Electric assisted front steering
EMB	Electromechanical brake (wedge)
SBW	Shift-by-wire
HVAC	Air compressor for air conditioner
FC-AC	Air compressor for fuel cells
EG	Electric gearbox
EHAS	Electro-hydraulic active suspension
EMAS	Electromechanical active suspension
EAT	Electrical assisted turbochargers
VVT	Variable valve timing
SG	Starter-generators
EV	Electric vehicle traction
HEV	Hybrid electric vehicle traction

I. Introduction

Steering systems – a classification

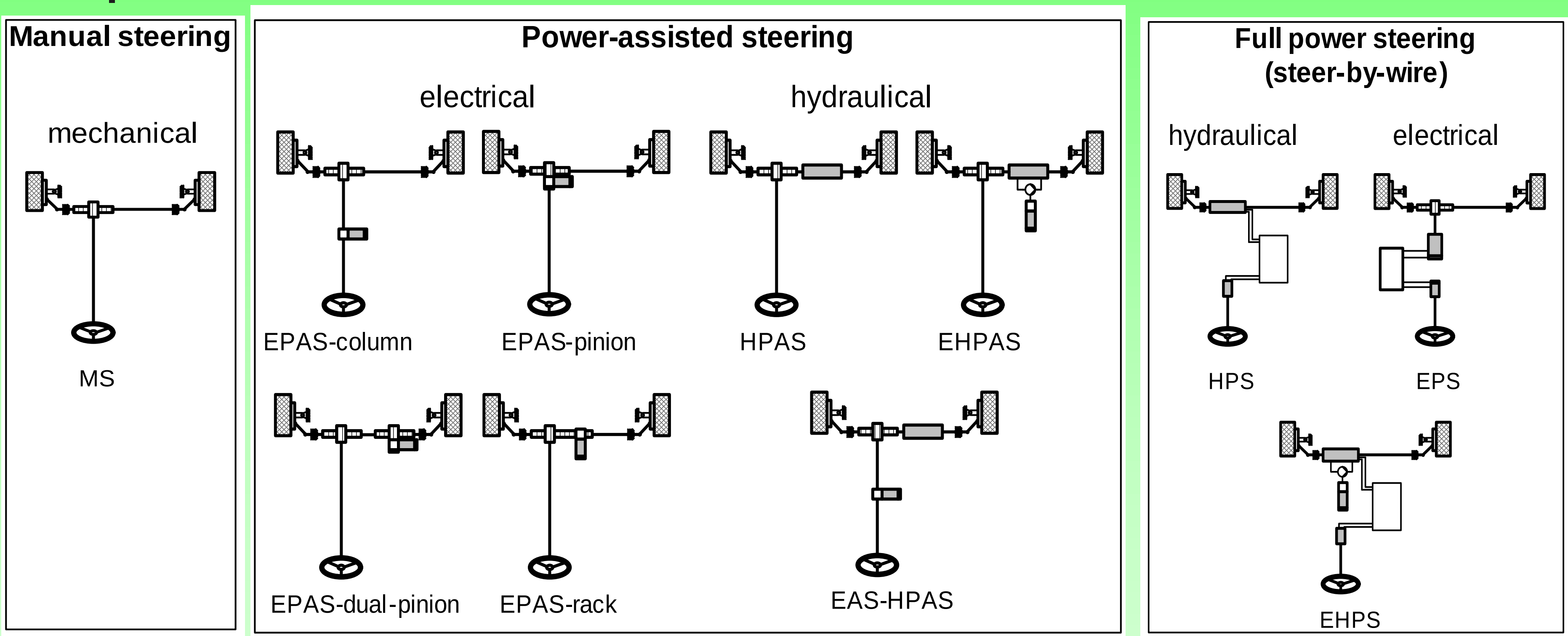

Steering parameters

- **steering torque (torque assistance)**
- **steering angle (angle assistance)**

I. Introduction

	DC	IM	PMSM BLDC	PMSM BLAC	SR	RS
Torque density	-	-	+	+	-	-
Torque/Amp	-	-	+	+	-	-
Peak to continuous torque capability	-	-	+	+	-	-
Variable speed control	+	-	-	-	-	-
Torque/inertia ratio	-	-	+	+	+	-
Energy efficiency	-	-	+	+	-	-
Speed range	-	+	-	-	+	+
Torque pulsations	-	+	-	+	-	+
Cogging torque	-	+	-	-	+	+
Temperature sensitivity (PM demagnetization)	-	+	-	-	+	+
Robustness	-	+	-	-	+	+
Fault tolerance Failure modes	+	-	-	-	+	-
Acoustic noise	-	+	-	+	-	+
Power converter requirements	+	-	-	-	-	-
Machine construction	-	-	+	+	+	+
Manufacturing technology	+	-	+	+	+	-
Reliability	-	+	+	+	+	+
Design and manufacturing experience	+	+	-	-	-	-
Customer acceptance	+	+	-	-	-	-
Motor cost	+	-	-	-	+	-
Drive system cost	+	-	+	-	-	-

Competing motor/drives technologies for automotive applications

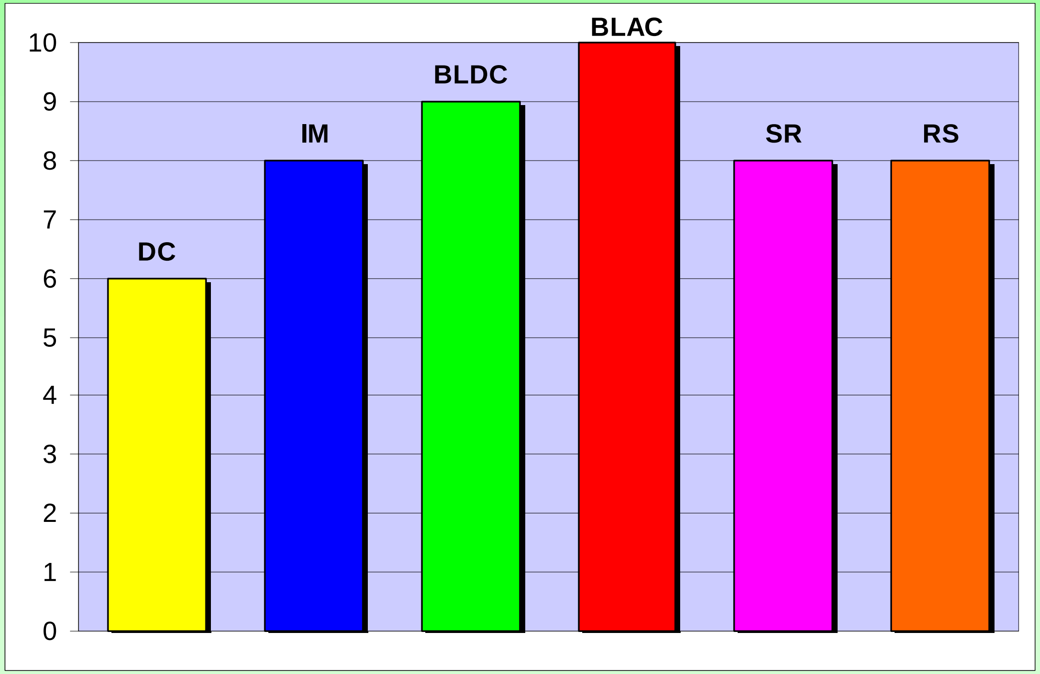

I. Introduction

PMSM-classification based on the shape of back-EMF and excitation currents

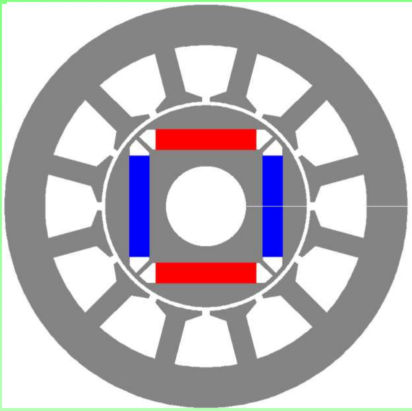

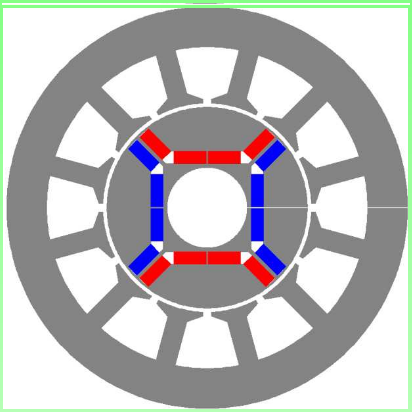

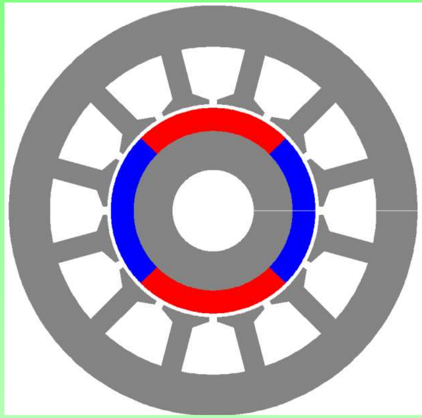

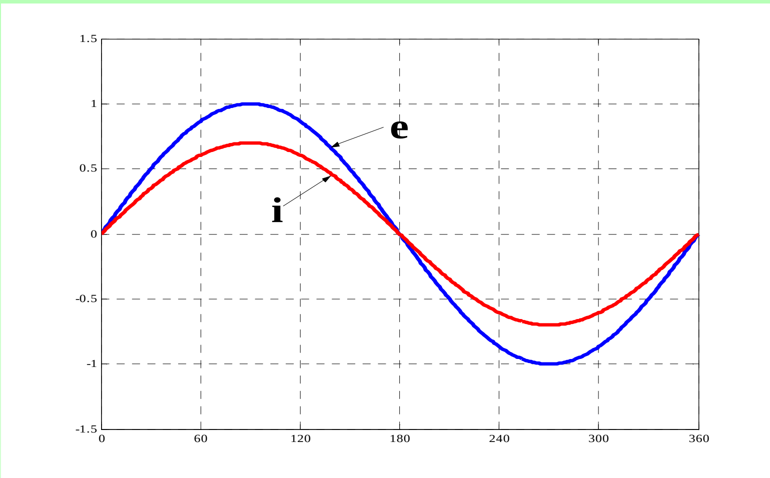

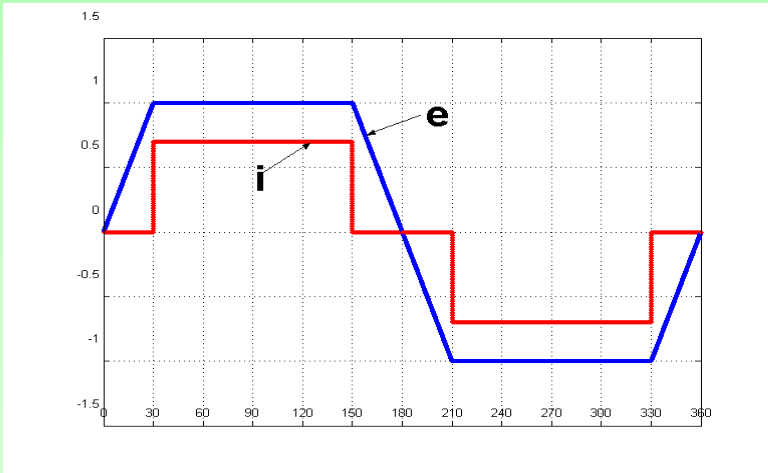

II.A. Defining the case study.

Schematics of an active front steering system:

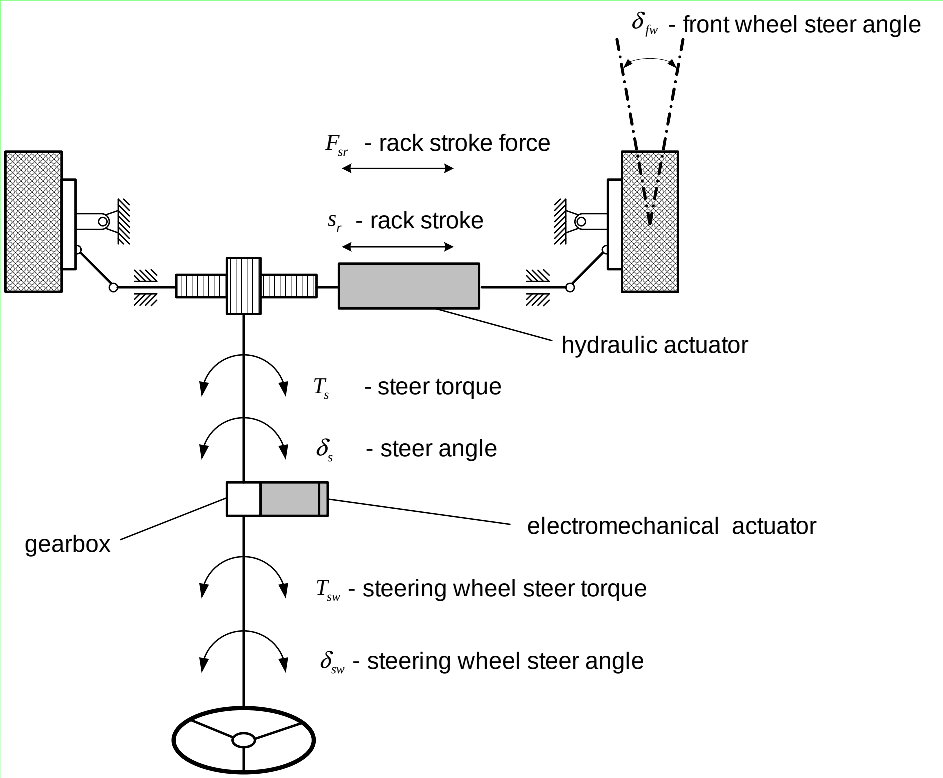

Motor specification data:

- $T_{en} = 1.14[Nm]$
- $n_n = 1000[rpm]$
- $V_{DC} = 12[V]$
- $T_{cogg} \leq 1\% \cdot T_{en}$
- $2p = 8$
- rectangular current control

II.A. Defining the case study.

Design solution:

- $D_{so} = 70[mm]$
- $D_{si} = 42[mm]$
- $g = 0.25[mm]$
- $l_{stack} = 20[mm]$
- $h_{PM} = 3[mm]$
- $w_{PM} = 13.75[mm]$

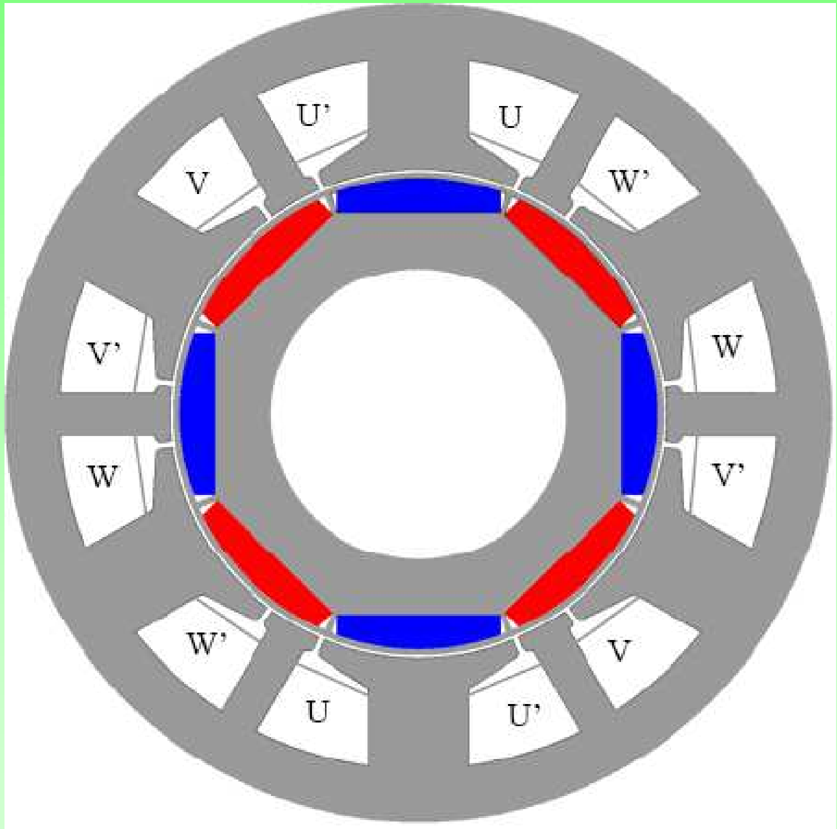

Motor cross-section

II.B. Materials, construction and manufacturing technologies

Winding layout of (6+6) slots/ 8 poles machine

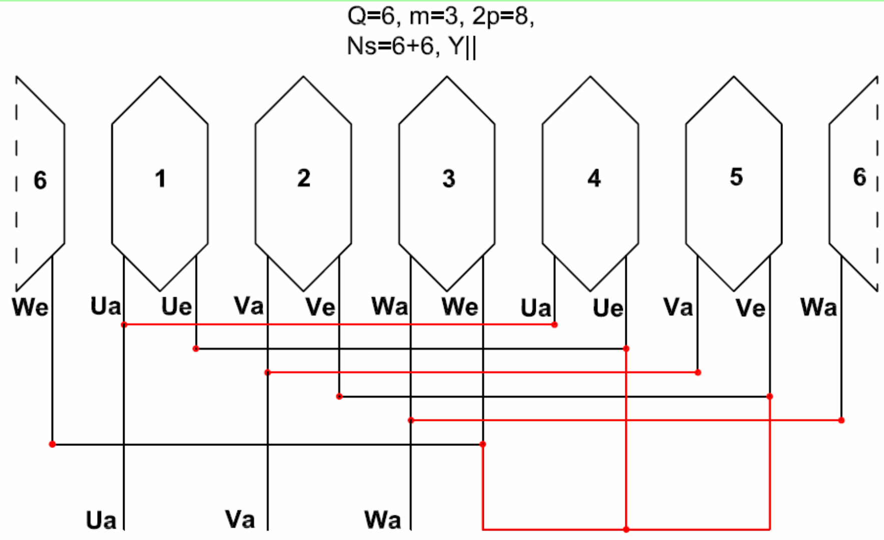

Stator and rotor before assembling

III. FEM characterization of BLDC using JMAG

Finite elements mesh

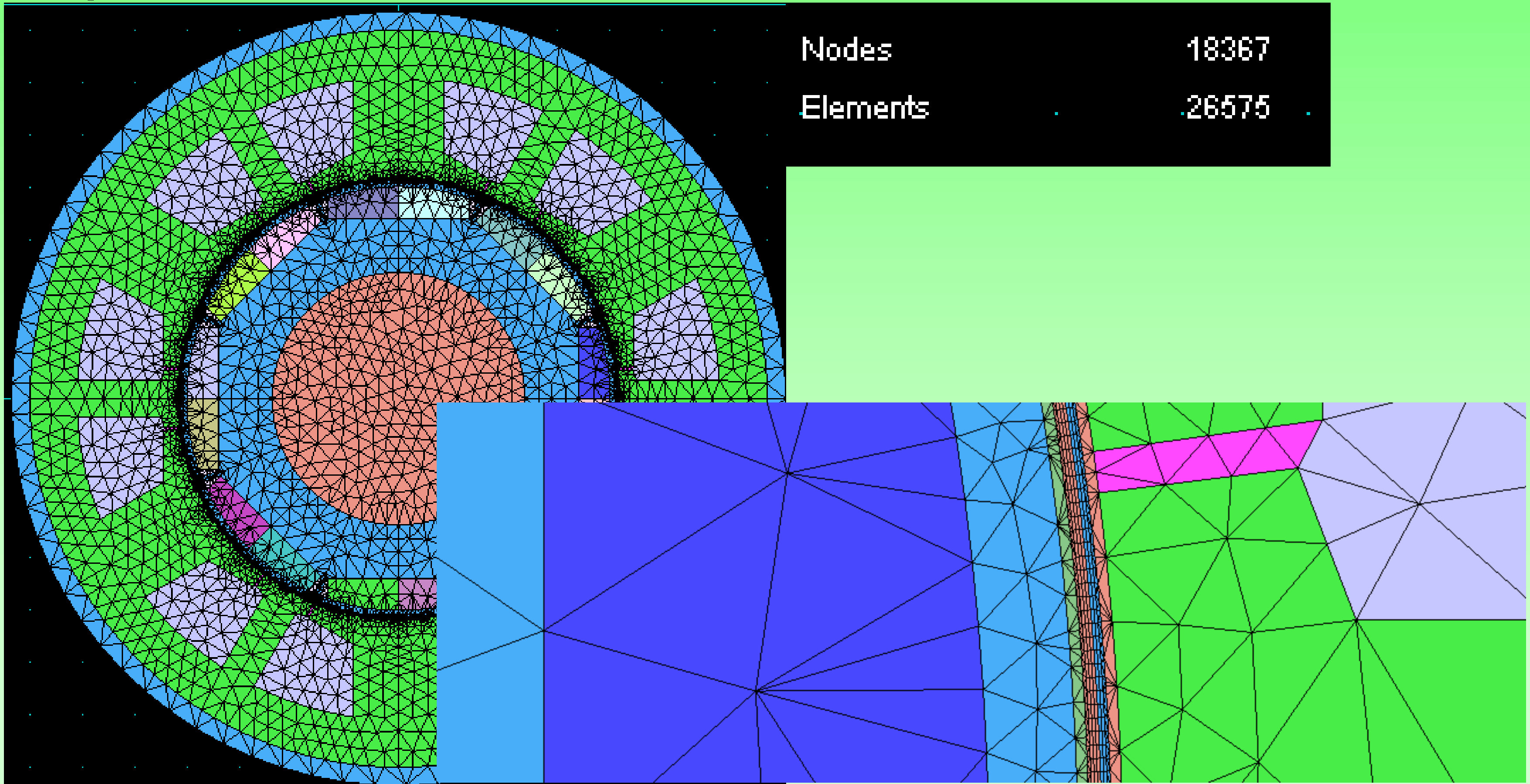

III. FEM characterization of BLDC.

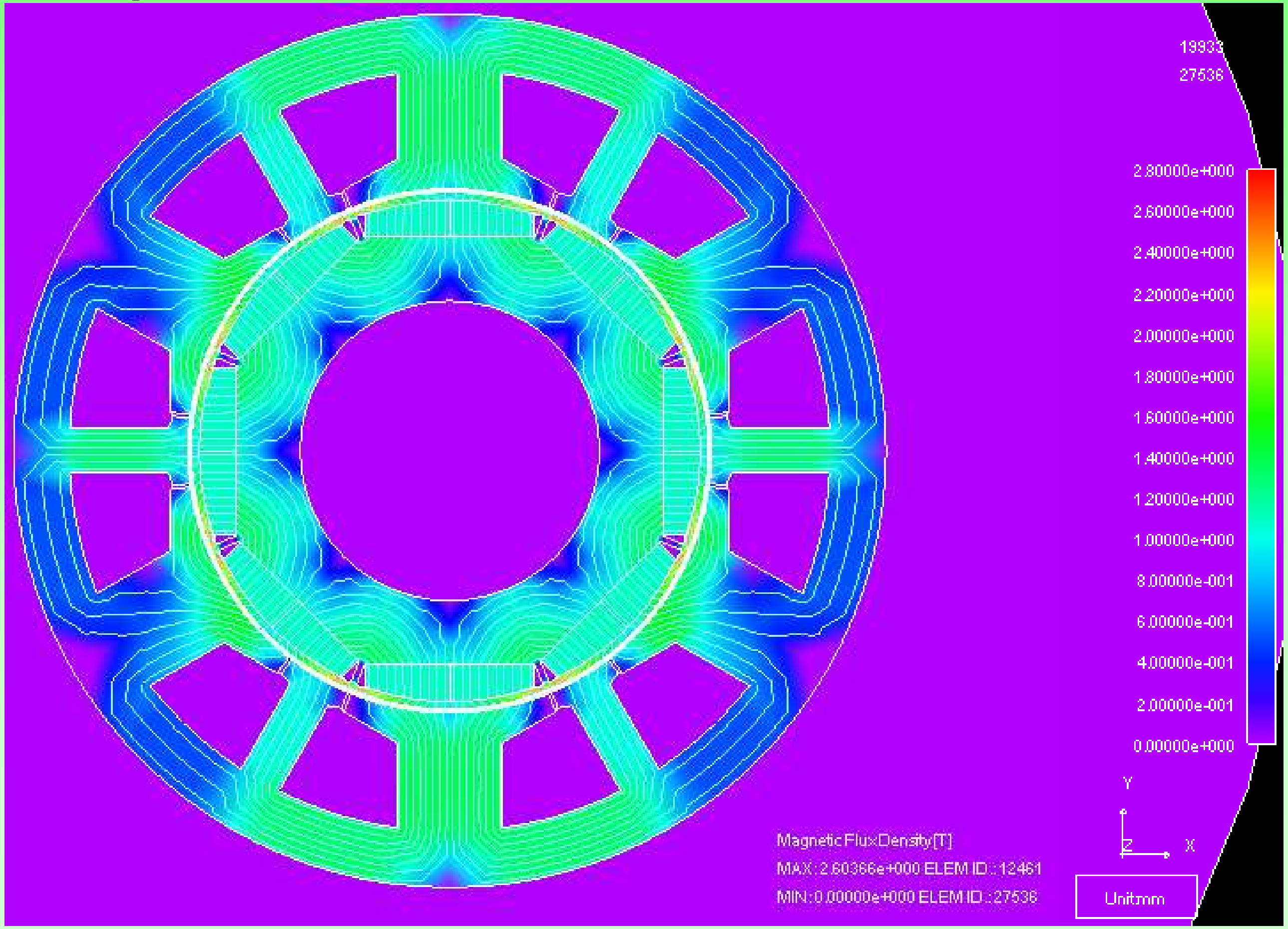

Magnetic loading
and flux lines
distribution
for the BLDC

III.A. Cogging torque calculation.

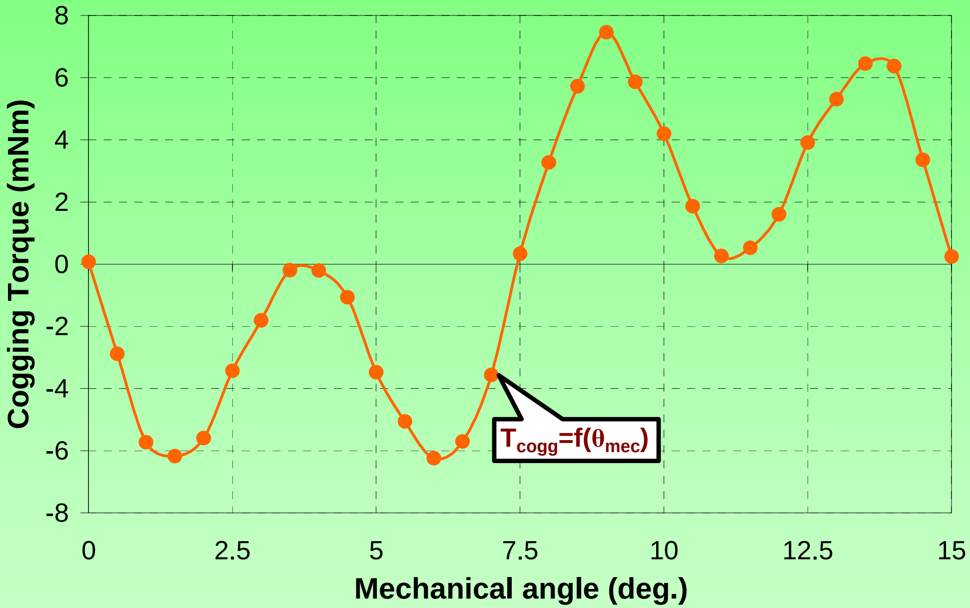

FEM-calculated cogging torque

For this topology, the minimization of cogging torque was done directly without skewing the slots:

$$T_{\max cogging} = 7.46\left[mNm\right] < 0.7\% \cdot$$

III.B. No load flux linkage and back-emf.

The back-EMF was calculated with:

$$E = -\frac{d\Psi}{dt} = -\frac{d\Psi}{d\theta_e} \cdot \frac{d\theta_e}{dt} = -\frac{d\Phi}{d\theta_e} \cdot n_c \cdot \frac{d\theta_{er}}{dt} = k_E \cdot \omega_r$$

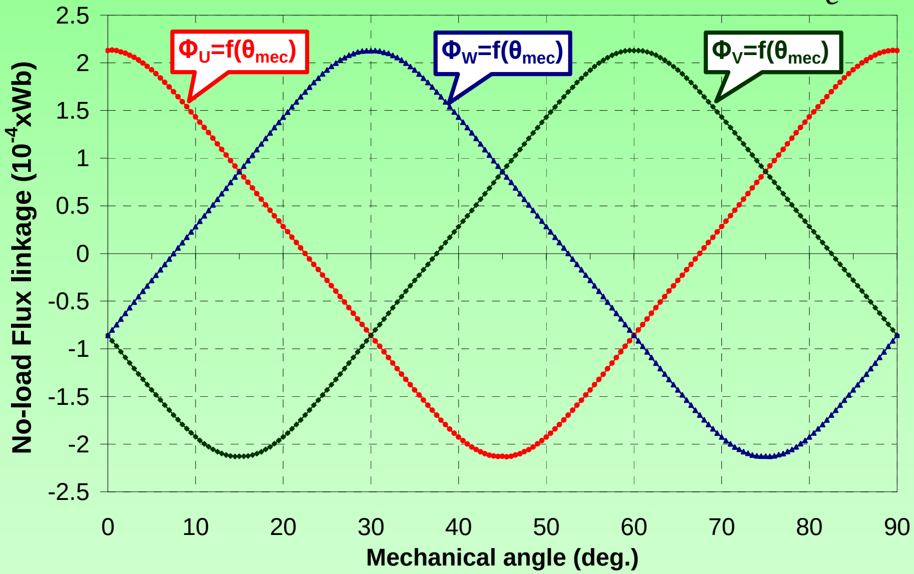

FEM-calculated no-load phase flux linkage

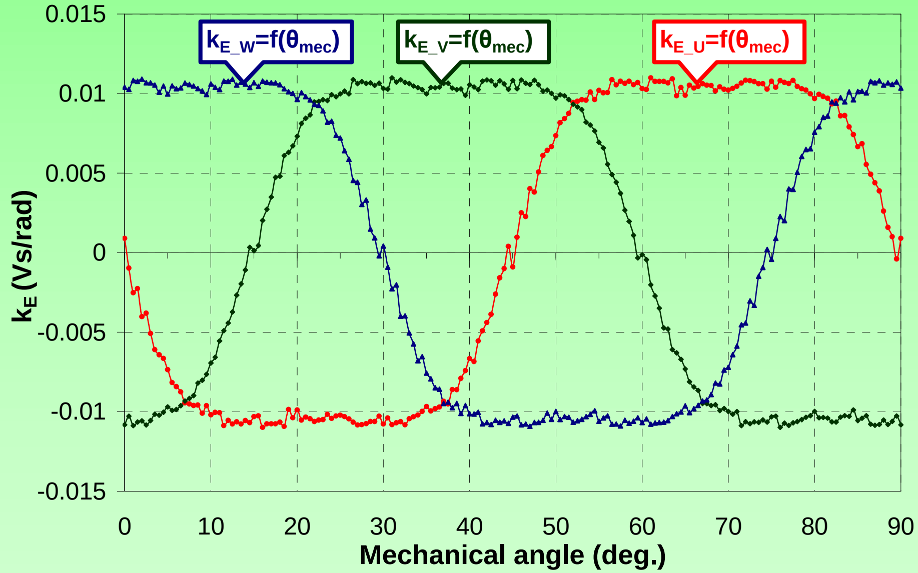

FEM-calculated phase back-EMF constant k_E versus rotor angular position

III.C. Load torque

Total torque vs. rotor angular position for four different phase current amplitudes

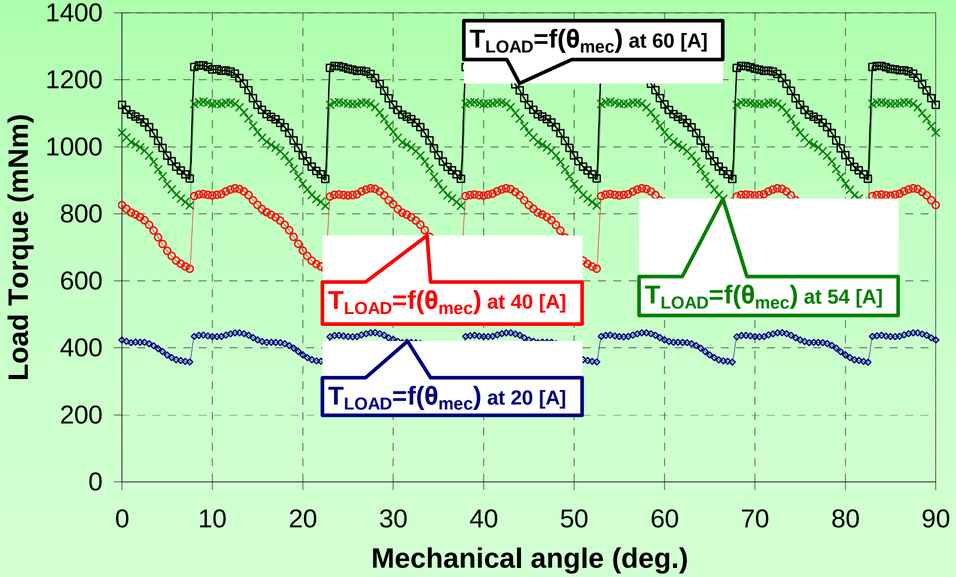

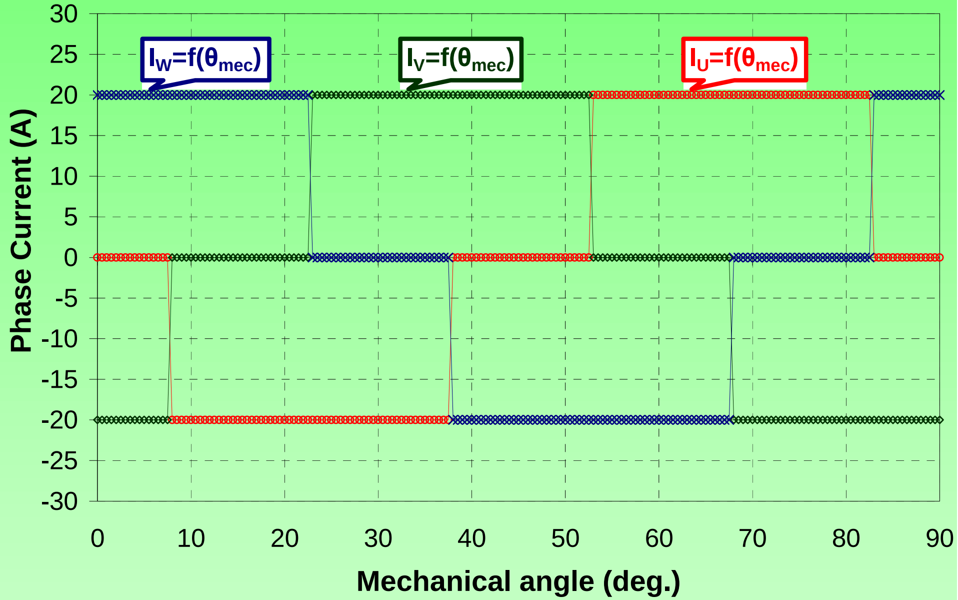

The rectangular waveforms of the phase currents

III.D. Computation of inductances

The inductance is calculated as a ratio of the flux linkage and the current:

$$L = \Psi / I$$

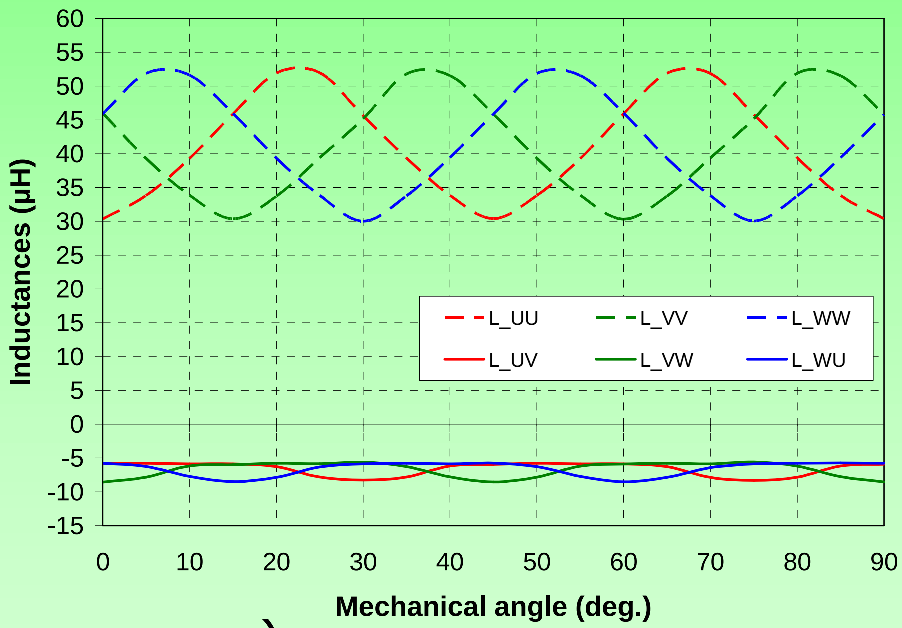

a)

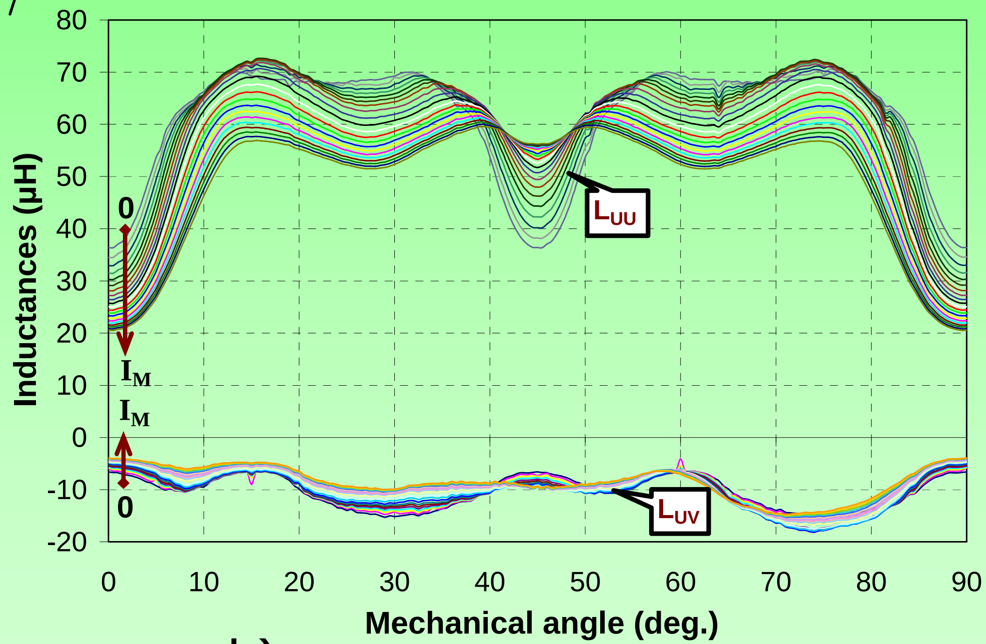

b)

Self and mutual FEM-calculated inductances for:
a) 28.3 [mA] ,b) L_{UU} and L_{UV} for I_U=(0 to I_M=34 A)

IV. Experimental analysis of IPMBLDC.

The measurement procedure consists of several tests. These tests where chosen in order to allow the estimation of machine parameters in a wide area of variation.

A first classification would subdivide them in standstill or locked-rotor, and running tests [9].

Whenever possible, the experimental characteristics are compared with FEM-calculated characteristics, in order to validate the FEM accuracy in determining the BLDC parameters.

IV.A. Phase resistance measurement.

This prototype presents a small asymmetry, 2.73%, of the phase resistances. The line-to-line resistances have an asymmetry of 1.21 %. For the industrial practice a phase resistance asymmetry of up to 3% is satisfactory [9].

Table III.
Resistance measurement results at 20 [^{0}C]

R_{ph} [mΩ]			Difference in comparison with mean value.		
U	V	W	%		
10.7	11.3	11	-2.73	2.73	0.00
11.00					
R_{LL} [mΩ]			Difference in comparison with mean value.		
UV	VW	WU	%		
22	22.2	21.7	0.15	1.06	-1.21
21.97					

For further parameter estimation the mean values of the phase and line-to-line resistances will be used.

IV.B. Phase self and line-to-line inductance measurement.

The measurement was done using a frequency of 50 Hz for the injected current. However, the inductances measured with this method are unsaturated values, as the injected current was very small (40 mApeak).

After measuring the phase self and line-to-line inductances, the mutual inductances for the Y-phase connection can be calculated with the formula:

$$L_{UV}(\theta_e) = \frac{L_{UU}(\theta_e) + L_{VV}(\theta_e) - L_{LL\_UV}(\theta_e)}{2}$$

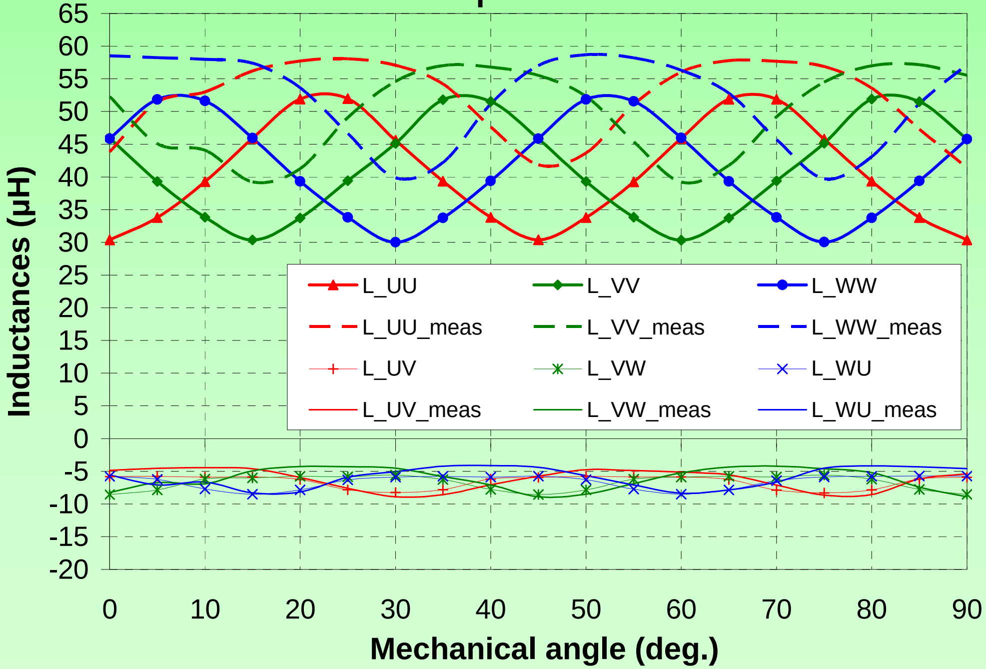

Phase self inductances measured with RLC-bridge (50 Hz, 40 mApeak) and mutual inductances in comparison with FEM-calculated ones.

IV.C. Standstill torque measurement.

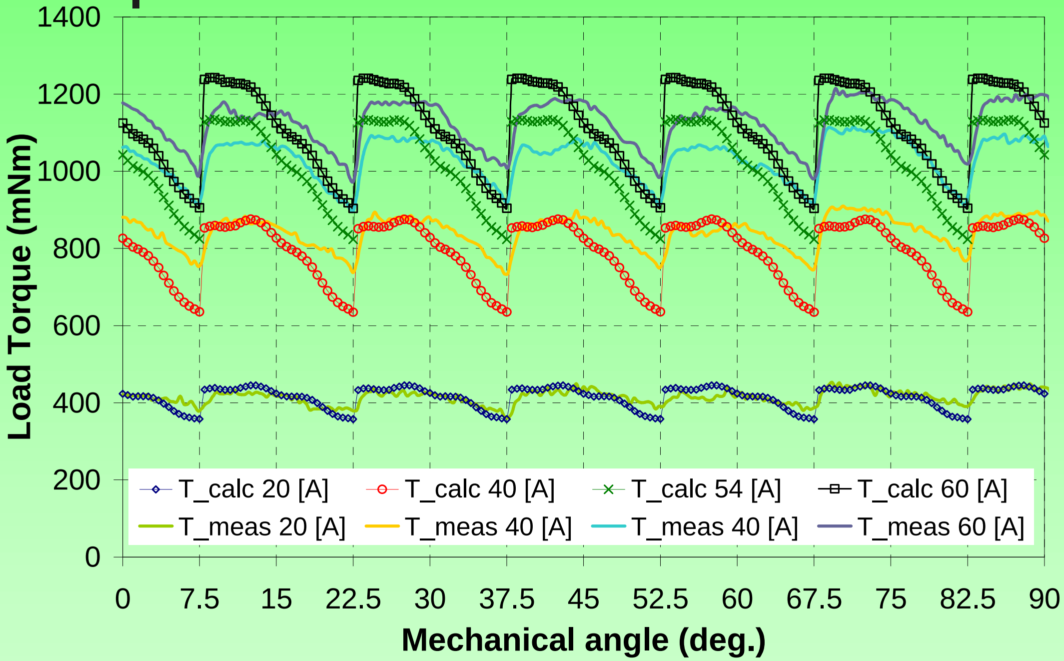

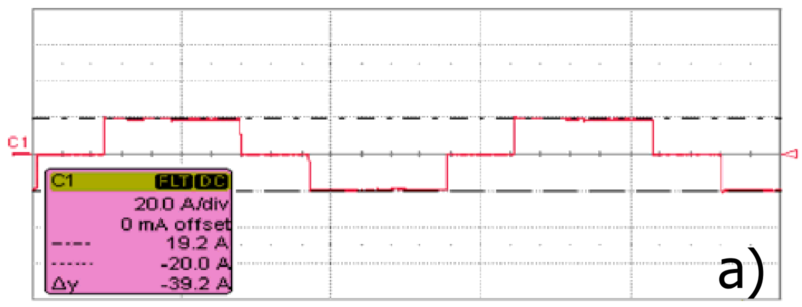

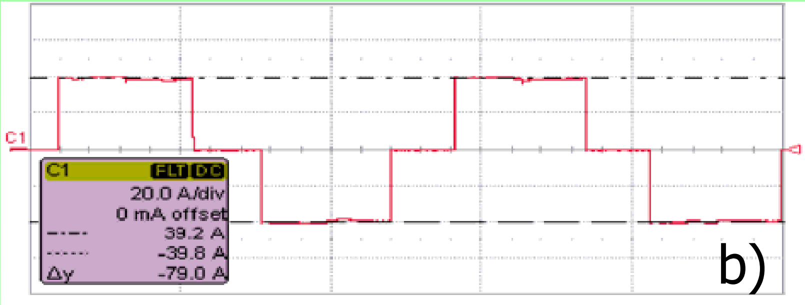

Measured and FEM-calculated torque vs. rotor position for four different phase current amplitudes

Phase current at:

a) 20 A amplitude, b) 40 A amplitude

(Measured during standstill torque measurements).

IV.D. Phase back-emf measurement.

The measurements were done running the machine as generator with open phases.

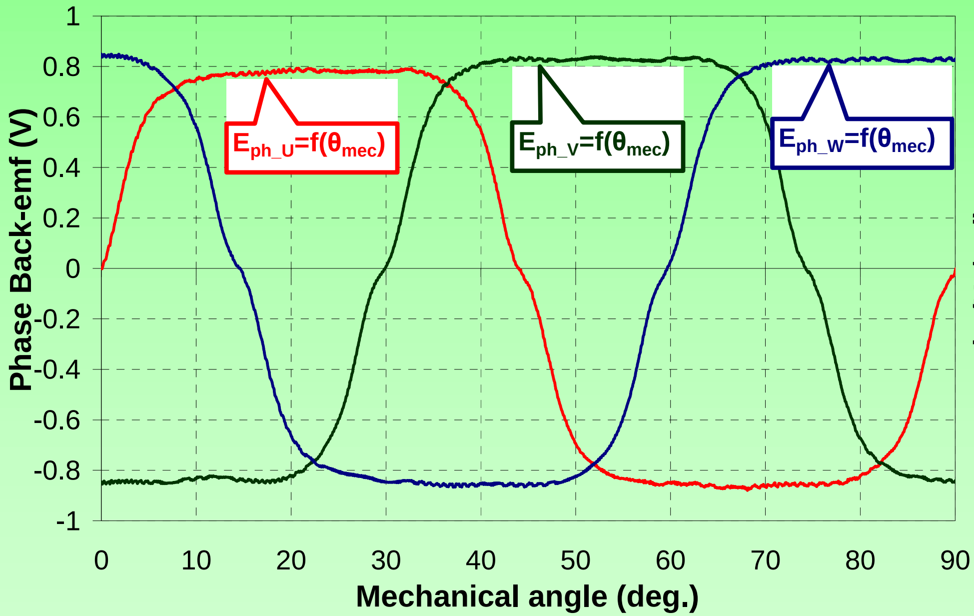

Shape of the phase back-emf (back-emf vs. rotor angular position at 750 rpm).

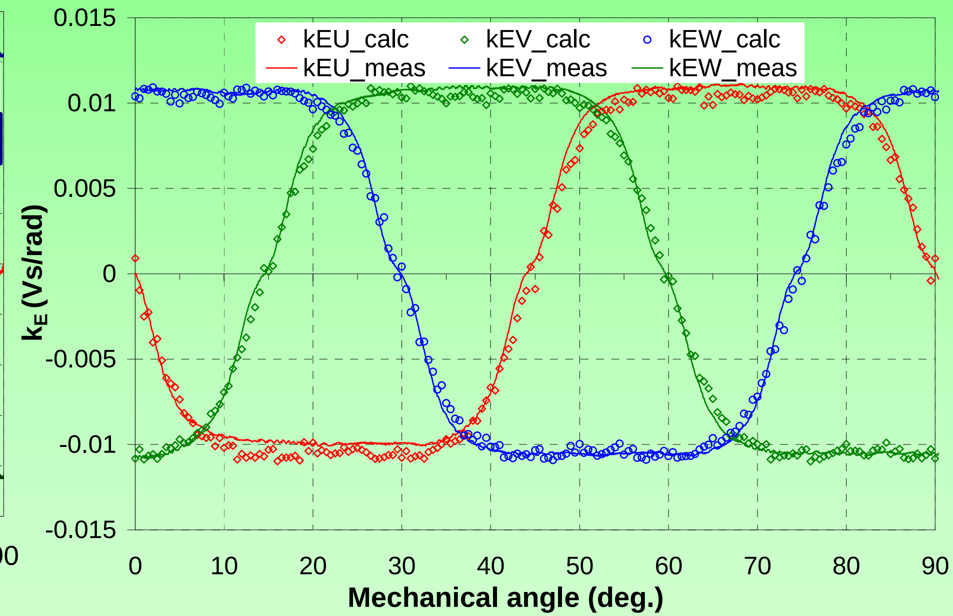

Measured and FEM-calculated back-emf constant k_{E_ph} vs. rotor angular position.

IV.E. Cogging torque measurement.

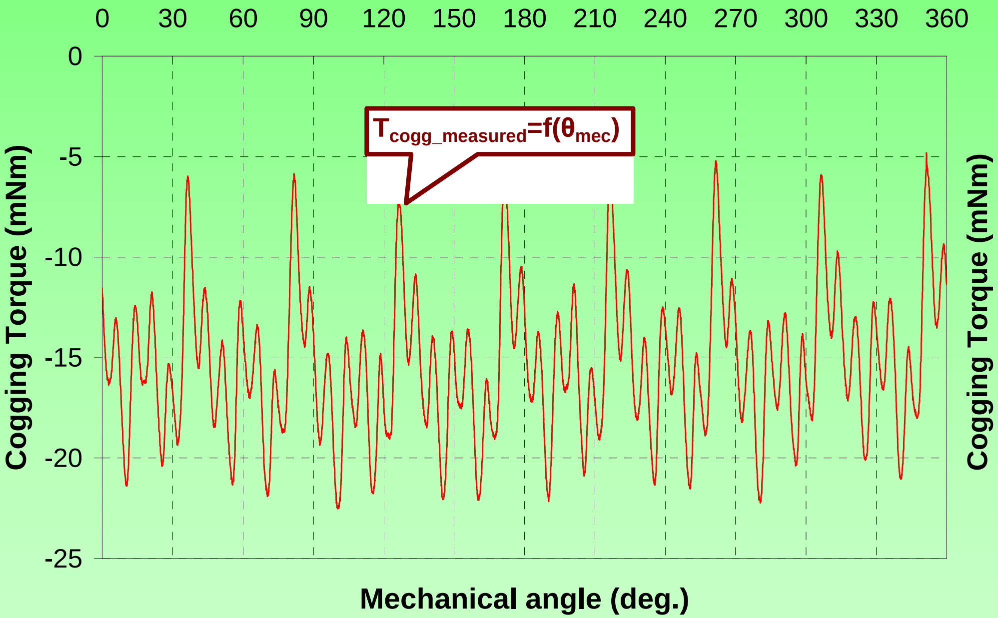

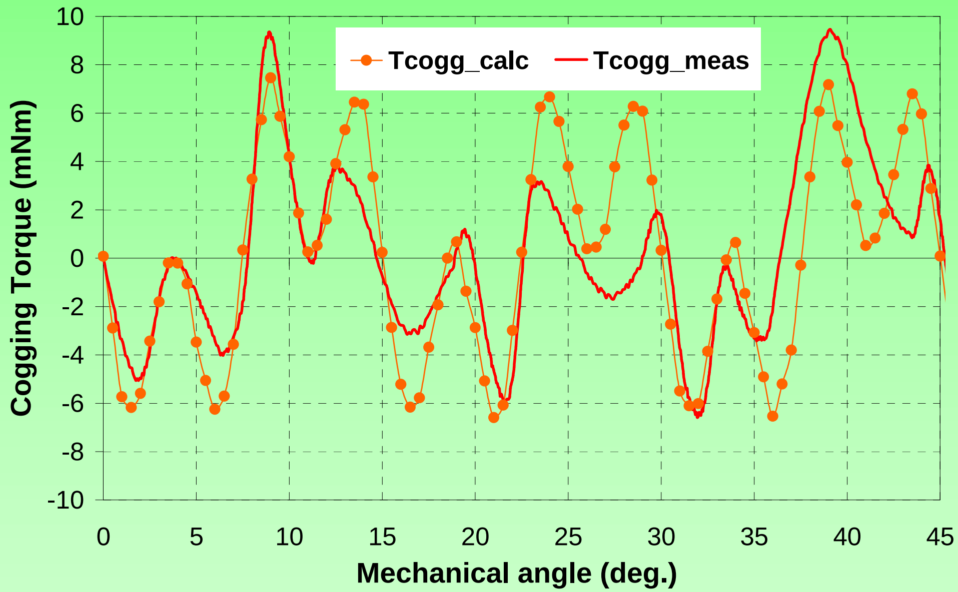

Measured cogging torque vs. rotor mechanical position angle

Measured cogging torque and FEM-calculated one vs. rotor mechanical position angle

IV.F. Friction and iron loss torque versus speed.

Measured iron and friction losses torque vs. speed

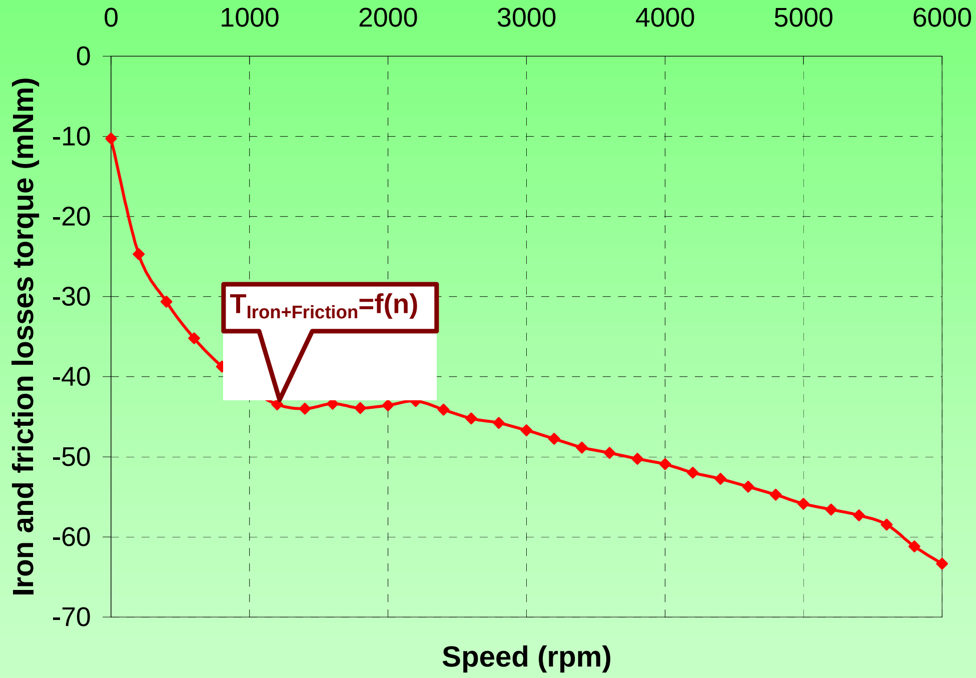

In order to separate the two torque components a measurement of the friction loss torque versus speed must be carried out. This would be possible only if the permanent magnets were removed from the rotor [9].

Conclusion

The IPM BLDC was considered as a proper candidate for an automotive actuator, due to the following advantages:

- concentrated coils, which provide lower copper losses [1], and lower manufacturing costs
- a very low cogging torque obtained directly without skewing the slots
- a simplified production of the rotor in comparison with surface PMSM, due to the simple shape and fixture of the permanent magnets.

A comparison between FEM-calculated and measured parameters of an interior permanent magnet BLDC motor was presented. This comparison was done in order to validate the FEM-calculated parameters of the motor.

REFERENCES

[1] J. Cros and Ph. Viarouge, "Synthesis of high performance PM motors with concentrated windings", *IEEE Transactions on energy conversion*, Vol. 17, No. 2, June 2002, pp. 248-253.

[2] J.-H. Choi, S.-H. You, J. Hur, and H.-G. Sung, "The Design and Fabrication of BLDC Motor and Drive for 42V Automotive Applications", *ISIE*, June 2007, pp. 1086-1091.

[3] S. Waikar, T. Gopalarathnam, H.A. Toliyat, and J. C. Moreira, "Evaluation Of Multiphase Brushless Permanent Magnet (BPM) Motors Using Finite Element Method (FEM) and Experiments", *APEC*, Vol. 1, March 1999, pp. 396-402.

[4] S. F. Gorman, C. Chen, and J. J. Cathey, "Determination of permanent magnet synchronous motor parameters for use in brushless d.c. motor drive analysis", *IEEE Transactions on Energy Conversion*, Vol. 3, No. 3, Sept. 1988, pp.674-681.

[5] K. M. Rahman, and S. Hiti, "Identification of Machine Parameters of a Synchronous Motor", *IAS*, Vol. 1, Oct. 2003, pp. 409-415.

[6] C. Grabner, "Idea, realization and characteristics of a novel permanent magnet motor topology with higher harmonic airgap waves in the BLDC mode", *ISIE*, June 2007, pp. 1056-1061.

[7] M. S. Islam, S. Mir, and T. Sebastian, "Paralleling the Stator Coils in Permanent Magnet Machines", *IEMDC*, May 2005, pp. 1479-1486.

REFERENCES

[8] T. Noguchi, "Trends of Permanent-magnet Synchronous Machine Drives", *IEEJ Transactions on Electrical and Electronic Engineering*, 2007, pp. 125-142.

[9] D. Iles-Klumpner, *Automotive Permanent Magnet Brushless Actuation Technologies*, PHD Thesis, University Politehnica Timisoara, Romania, 2005.

[10] A. Ştirban, L. Tutelea, D. Iles-Klumpner, and I. Boldea, "FEM analysis of concentrated coils nonuniform slot (6+6/8) IPMSM fed with trapezoidal current", *OPTIM*, 2008, pp. 45-52.

[11] D. Iles-Klumpner, I. Şerban, M. Risticevic, and I. Boldea, "High-Speed Automotive Permanent Magnet Synchronous Motors", *Proceedings of PCIM*, 2005, Nürnberg, Germany.

[12] M. Kondo, "Parameter Measurements for Permanent Magnet Synchronous Machines", *IEEE Transactions on Electrical and Electronic Engineering*, 2007, pp. 109-117.

[13] T. J. E. Miller, M. Popescu, C. Cossar, and M. McGilp, "Performance Estimation of Interior Permanent-Magnet Brushless Motors Using the Voltage-Driven Flux-MMF Diagram", *IEEE Trans. On Magnetics*, Vol. 42, No. 7, July 2006, pp. 1867-1872.

- **http://www.youtube.com/watch?v=umsULUG2P-M**